

# The case against the progenitor's carbon-to-oxygen ratio as a source of peak luminosity variations in Type Ia supernovae

F. K. Röpke<sup>1</sup>, and W. Hillebrandt<sup>2</sup>

<sup>1</sup> Max-Planck-Institut für Astrophysik, Karl-Schwarzschild-Str. 1, D-85741 Garching, Germany  
e-mail: fritz@mpa-garching.mpg.de

<sup>2</sup> e-mail: wfh@mpa-garching.mpg.de

the date of receipt and acceptance should be inserted later

**Abstract.** One of the major challenges for theoretical modeling of Type Ia supernova explosions is to explain the diversity of these events and the empirically established correlation between their peak luminosity and light curve shape. In the framework of the so-called Chandrasekhar mass models, the progenitors carbon-to-oxygen ratio has been suggested to be a principal source of peak luminosity variations due to a variation in the production of radioactive  $^{56}\text{Ni}$  during the explosion. The underlying idea is that an enhanced carbon mass fraction should result in a more vigorous explosion since here the energy release from nuclear reactions is increased. It was suspected that this would produce a higher amount of  $^{56}\text{Ni}$  in the ejecta. In this letter we describe a mechanism resulting from an interplay between nucleosynthesis and turbulent flame evolution which counteracts such an effect. Based on three-dimensional simulations we argue that it is nearly balanced and only minor differences in the amount of synthesized  $^{56}\text{Ni}$  with varying carbon mass fraction in the progenitor can be expected. Therefore this progenitor parameter is unlikely to account for the observed variations in Type Ia supernova luminosity. We discuss possible effects on the calibration of cosmological measurements.

## 1. Introduction

The question of the origin of the observed diversity of Type Ia supernovae (SNe Ia) has been a long standing problem. Although these astrophysical events possess a surprising homogeneity of features, which led to the application of SNe Ia as distance indicators in cosmology, variations of photometric and spectroscopic data have been reported. Nevertheless, corrections of the luminosity based on an empirical relation between peak luminosity and light curve shape (Phillips, 1993) made SNe Ia a major tool of observational cosmology (for a recent review see Leibundgut 2000). A theoretical understanding of this correlation is still lacking. Thus the challenge for astrophysical theory is to construct a SN Ia explosion model that is robust and—as a first step—able to explain the observed variations.

It is generally agreed on the fact that SNe Ia originate from thermonuclear explosions of white dwarf (WD) stars, although many scenarios have been proposed for the particular realization (see Hillebrandt & Niemeyer (2000) for a recent review). The currently favored model is a binary system in which a WD composed of carbon and oxygen accretes matter from a non-degenerate companion until it reaches the Chandrasekhar mass. At this point, thermonuclear burning at the center of the star develops into a flame which propagates outward. From the viewpoint of hydrodynamics, two modes of flame propagation are

possible: a subsonic deflagration, in which the reaction is mediated by thermal conduction of the degenerate electrons, and a supersonic shock-induced detonation. Arnett (1969) noted that to produce the observed intermediate mass elements a prompt detonation can be excluded. Therefore the flame starts out in the deflagration mode and may or may not develop into a detonation. The key feature of this model is that buoyancy-induced instabilities lead to a turbulization of the flame front in the deflagration mode. Only due to this effect the flame is accelerated sufficiently to power SN Ia explosions.

In the first stages the prevailing densities and temperatures are high enough that the reaction terminates in nuclear statistical equilibrium (NSE), consisting mainly of iron group elements. As the WD expands, density and temperature drop and the thermonuclear reactions produce intermediate mass elements such as Si, S, and Ca.

The light curve of SNe Ia is powered by the radioactive decay of  $^{56}\text{Ni}$  and  $^{56}\text{Co}$ . The peak luminosity is a measure of the  $^{56}\text{Ni}$  produced by the explosion (“Arnett’s law”, Arnett 1982). Parameters that have frequently been suggested to affect the amount of  $^{56}\text{Ni}$  synthesized are the carbon-to-oxygen (C/O) ratio of the WD, its central density prior to ignition, and its metallicity. Of course, other parameters like rotation and asphericity of the explosion may play a role, too. A thorough investigation of the impact of these parameters is mandatory for the validation of cosmological measurements, since here possible evolution effects with cosmic age are critical.

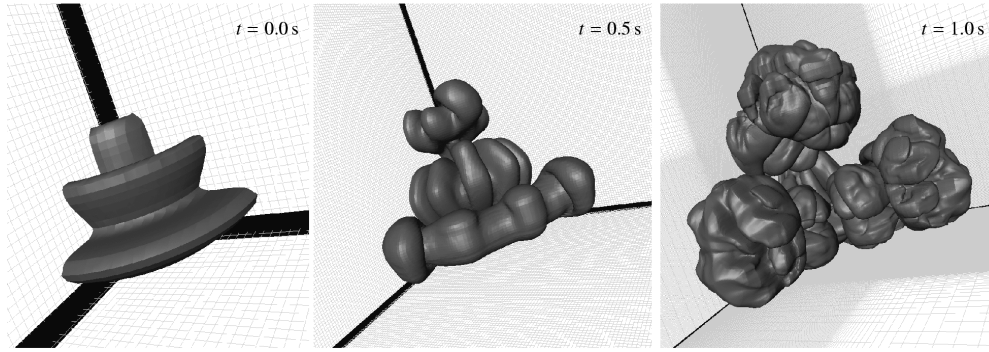


**Fig. 1.** Temporal evolution of the burning front.

The objective of the present study is to explore the effect of the progenitor’s C/O ratio on the supernova explosion by means of three-dimensional hydrodynamical models. Since we are mainly interested in the explosion energy and the amount of synthesized  $^{56}\text{Ni}$ , it is justified to focus on the deflagration stage, leaving aside a possible delayed detonation. Only in this first stage of the SN Ia explosion the prevailing densities and temperatures are sufficient for burning to iron group elements, and therefore the main part of the  $^{56}\text{Ni}$  and probably also of the explosion energy is produced here.

## 2. The numerical model

The numerical model applied to simulate the thermonuclear explosion is the same as used for several studies by Reinecke et al. (2002a,b). Therefore we will be short in the description of the model and only mention the basic aspects here.

The vast range of involved length scales makes fully resolved SN Ia explosion simulations impossible. Therefore we describe the flame propagation by applying the level set method (Osher & Sethian, 1988). Neither the internal flame structure nor its wrinkling on small scales are resolved but the flame is rather modeled as a discontinuity separating fuel and ashes. This discontinuity represents the mean position of the flame. To track its propagation it is associated with the zero level set of a scalar field  $G$  which is evolved according to the scheme described by Reinecke et al. (1999). In this scheme the effective flame velocity must be provided and for this we employ the subgrid scale model proposed by Niemeyer & Hillebrandt (1995) which describes the effects of the turbulent motions on unresolved scales. The hydrodynamics is modeled based on the PROMETHEUS implementation (Fryxell et al., 1989) of the piecewise parabolic method (Colella & Woodward, 1984).

Due to the restricted computational resources only a very simplified description of the nucleosynthesis is possible concurrent with the explosion simulation. We follow the approach suggested by Reinecke et al. (2002a), who include five species, namely  $\alpha$ -particles,  $^{12}\text{C}$ ,  $^{16}\text{O}$ ,  $^{24}\text{Mg}$  as a representative of intermediate mass elements and  $^{56}\text{Ni}$  as a representative of iron group nuclei (denoted as “Ni” in the following to avoid confusion with the particular isotope as part of the ejecta). The fuel is assumed to consist of a mixture of carbon and oxygen. At the initially high densities burning proceeds to NSE composed of  $\alpha$ -particles and “Ni”. Depending on temperature and den-

**Table 1.** Characteristics of the explosion models.

$X(^{12}\text{C})$	$E_{\text{nuc}}$ [ $10^{50}$ erg]	$M(\text{“Ni”})$ [ $M_{\odot}$ ]	$\max(M_{\alpha})$ [ $M_{\odot}$ ]
0.30	8.85	0.5178	0.04579
0.46	9.46	0.5165	0.05177
0.62	9.97	0.5104	0.05636

sity in the ashes, the amount of  $\alpha$ -particles and nickel changes. Once the fuel density drops below  $5.25 \times 10^7 \text{ g cm}^{-3}$  due to the expansion of the WD, burning is assumed to terminate at intermediate mass elements and below  $1 \times 10^7 \text{ g cm}^{-3}$  burning becomes very slow and is not followed anymore.

In this letter we will present three simulations that span one octant of our coordinate system and assume mirror symmetry to the other octants. The simulations were set up on a cartesian computational grid that was equally spaced in the inner regions. In order to be able to follow the explosion for a longer period of time in the outer parts the width of the grid cells was expanded exponentially.

The resolution of the runs was rather low—the computational domain was divided in  $[256]^3$  grid cells corresponding to a central grid resolution of  $10^6 \text{ cm}$ . In each direction the grid length in the outer 35 zones was increased subsequently by a factor of 1.15. The burning was centrally ignited and the spherical initial flame structure was perturbed with three toroidal rings per octant (see also Fig. 1).

## 3. Results of three-dimensional explosion models

Snapshots from the explosion simulation for  $X(^{12}\text{C}) = 0.46$  are given in Fig. 1. Here the position of the flame front is rendered as represented by the zero level set of the scalar field  $G$  dividing fuel and ash. The spatial extent of the burnt region can be inferred from the plotted grid which also visualizes our setup with uniform grid cells in the inner region and an exponential growth of the grid spacing further out. The flame as initialized in our setup is shown in the left snapshot of Fig. 1. In the subsequent images the growth of instabilities and an increasing wrinkling of the flame front is visible.

To test the effect of a varying carbon mass fraction of the WD, we performed three simulations with values of  $X(^{12}\text{C})$  given in Table 1. Figure 2 shows snapshots from models with different  $X(^{12}\text{C})$  after 1.0 s. It is essential for the following

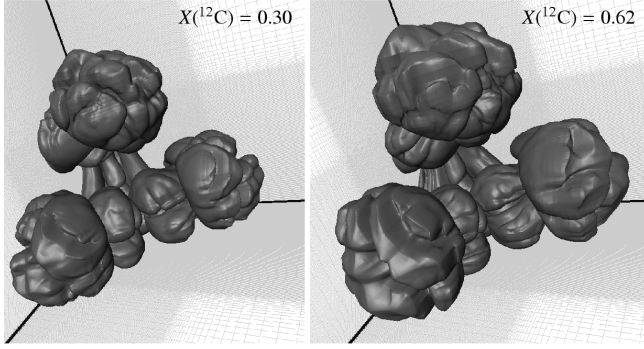


**Fig. 2.** Flame front at  $t = 1.0$  s for models with different carbon mass fraction of the progenitor material.

argumentation to note that for all three models the extent of the burnt region and also the flame morphology are surprisingly similar. The latter is in agreement with the findings of Gamezo et al. (2003), but Khokhlov (2000) claims that a decreasing  $X(^{12}\text{C})$  would result in weaker explosions because of a delay of the development of the Rayleigh-Taylor instability, which seems to be only a minor effect in our simulations.

The energy release of the different models are summarized in Table 1. Obviously, a higher carbon mass fraction leads to a higher total energy production for fixed central densities. This trend is not surprising. For larger  $X(^{12}\text{C})$  the laminar burning velocity increases (Timmes & Woosley, 1992). This effect, however, will be important only in the earliest stages of the explosion, since flame propagation becomes determined by turbulence shortly after ignition and can therefore only account for minor changes. More significant, a higher carbon mass fraction will increase the total energy generation for the simple reason that the binding energy of  $^{12}\text{C}$  is lower than that of  $^{16}\text{O}$  so that it releases more energy by fusion to “Ni”.

Therefore the very similar flame evolution of all models is not expected in a simple picture. That this is nevertheless the case is corroborated by the following arguments. As mentioned in Sect. 1, the flame evolution in the deflagration mode is dominated by turbulization which results from Rayleigh-Taylor-like instabilities. An important parameter for this is the effective gravity experienced by the flame. It accelerates the development of flame structures resulting from the non-linear stage of the Rayleigh-Taylor instability. At early stages the energy fed into the turbulent cascade from the interfaces of large scale buoyant burning bubbles will be enhanced by a higher  $g$ . Thus, the turbulent cascade will develop more quickly and the turbulence-induced boost of the effective flame propagation velocity sets in earlier.

Our models, however, do not show such a behavior. In Fig. 3 the temporal evolution of the mean  $g$  experienced by the flame is plotted. We note only small differences for varying  $X(^{12}\text{C})$ . This results in a very similar evolution of the turbulent energy in our models.

The mechanism that is responsible for the reduced effect of the varying carbon mass fraction on the flame propagation becomes plausible from the evolution of the chemical composition of our models (see Fig. 4). Though the temporal evolution

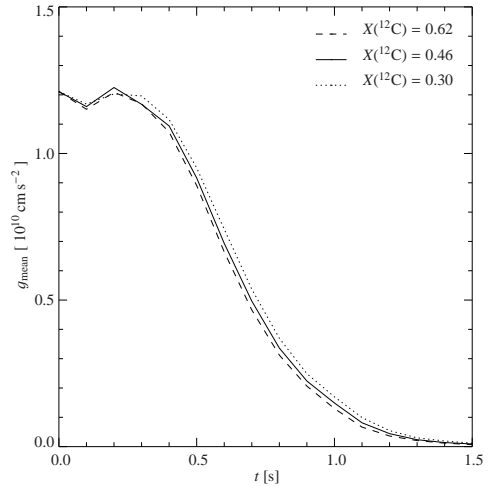


**Fig. 3.** Mean gravitational acceleration  $g_{\text{mean}}$  experienced by the flame front for models with different carbon mass fraction of the progenitor material.

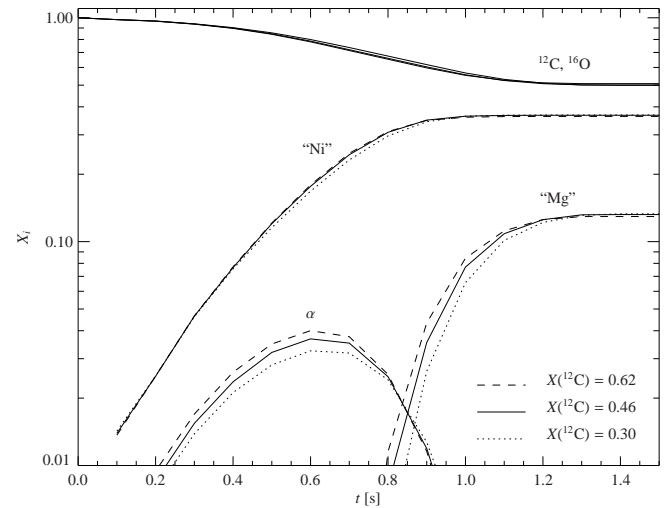


**Fig. 4.** Temporal evolution of the chemical composition in models with different carbon mass fraction of the progenitor material.

of the mass fractions of carbon and oxygen as well as nickel show little differences, the variations of the mass fractions of  $\alpha$ -particles and intermediate mass elements is significant.

As pointed out by Reinecke et al. (2002a), the abundance of  $\alpha$ -particles is important for the explosion dynamics. At high densities and temperatures the flame converts the C/O fuel to NSE which in our models is represented by a mixture of nickel (representing the iron group nuclei) and  $\alpha$ -particles. The  $\alpha$ -particles are produced at high temperatures in the ashes and have two effects. First, the binding energy of the ashes is lower in case of higher  $X(\alpha)$ , so less energy is released. Second, the number of particles per unit mass of the ashes increases and this decreases the temperature. Both effects result in a lower temperature and a higher density of the burning products which delays the expansion of the WD and decreases the buoyancy of the burnt regions. Thus the flame acceleration is lower and the

burning is suppressed. With further expansion of the WD, the  $\alpha$ -particles are converted to nickel.

In our simulations  $\alpha$ -particles are present between 0.2 s and 0.9 s. The maximal  $X(\alpha)$  is given in Table 1. Obviously, higher carbon mass fraction in the fuel gives rise to a larger fraction of  $\alpha$ -particles in the ashes. Therefore the evolution of the flame front is more delayed and consequently the explosion dynamics of the models in the first stage when the iron group elements are synthesized is comparable. The result of this effect is a production of similar amounts of iron group elements. The energy stored in the  $\alpha$ -particles is released at later times and the total energy released in the explosion models varies for about 12% while the mass of produced nickel differs only about 1.4% (cf. Table 1).

Note that the explosion energies and the masses of synthesized iron group elements in all our models are rather on the low side to explain a prototype SNe Ia. This is due to the low numerical resolution of our models. Although they are expected to be numerically converged (Reinecke et al., 2002c), the resolution does not allow to apply multi-spot ignition scenarios which have been shown to produce more vigorous explosions (Reinecke et al., 2002b). However, the trends inferred from our models are expected to be robust.

#### 4. Conclusions

In this letter we described a mechanism that is responsible for the somewhat surprising fact that although the progenitor's C/O ratio affects the energy release of SN Ia explosions, it has little effect on the peak luminosity determined by the  $^{56}\text{Ni}$  mass. This is found with help of three-dimensional simulations and disagrees with the results reported from one-dimensional models. Höflich et al. (1998) find a 14% decrease in  $M_{\text{Ni}}$  when reducing the C/O ratio from 1/1 to 2/3; the fact that they considered a delayed detonation model should not greatly affect the comparability for reasons given in Sect. 1. The “working hypothesis” of an increased  $^{56}\text{Ni}$  production with higher  $X(^{12}\text{C})$  established by Umeda et al. (1999) cannot be confirmed. The reason for this discrepancy is a complex interplay between nucleosynthesis and nonlinear flame evolution which can be modeled appropriately only in three dimensions. The models presented here are based on a rather simplistic description of the nuclear reactions, which will be improved in forthcoming models. Nevertheless, the features that are important for the explosion dynamics are taken into account and trends can be revealed with this approach.

An interesting question is how our results affect the peak luminosity–light curve shape relation of SNe Ia. Since no light curves were calculated from our models we can only speculate on the effects based on the trends found by Arnett (1982) and Pinto & Eastman (2000) by means of analytic studies. According to “Arnett’s law” the peak luminosity should reflect the amount of radioactive  $^{56}\text{Ni}$  synthesized in the explosion. Since in our models the evolution of the densities of the ashes are very similar, the little variation in the iron group elements will result in little variation of the  $^{56}\text{Ni}$  mass. Thus the peak luminosity should be roughly the same for our three models. The explosion energy, however, varies significantly and

a greater expansion at late stages of the explosion associated with a larger C/O ratio would result in a more rapid decline of the light curve but also in a somewhat higher luminosity. This is in contradiction to the empirically established relation that for brighter SNe Ia the light curve declines slower, which has been extensively applied to calibrate cosmological distance measurements.

Timmes et al. (2003) analytically found a linear dependence of the amount of produced  $^{56}\text{Ni}$  on the progenitor’s metallicity. This in turn is, however, not likely to affect the explosion energy and dynamics significantly. Of course, from the viewpoint of stellar evolution there is an interrelation between the progenitor’s metallicity and other parameters, including its carbon mass fraction. Therefore it is plausible that the “luminosity-width relation” is caused by a combination of different parameters and that a direct relation between the  $^{56}\text{Ni}$  mass and the peak luminosity might be oversimplified. It seems well possible that the distribution of the  $^{56}\text{Ni}$  due to three-dimensional effects plays an important role here. In a subsequent publication we will report on a systematic parameter study addressing these questions. Ultimately, SN Ia explosion models will have to be coupled to realistic stellar evolution of the progenitor system and the calculation of synthetic light curves becomes mandatory.

*Acknowledgements.* We thank M. Reinecke, C. Travaglio, M. Gieseler, and W. Schmidt for helpful discussions.

#### References

- Arnett, W. D. 1969, *Astrophys. Space Sci.*, 5, 180
- Arnett, W. D. 1982, *Astrophys. J.*, 253, 785
- Colella, P. & Woodward, P. R. 1984, *J. Comp. Phys.*, 54, 174
- Fryxell, B. A., Müller, E., & Arnett, W. D. 1989, *Hydrodynamics and nuclear burning*, MPA Green Report 449, Max-Planck-Institut für Astrophysik, Garching
- Gamezo, V. N., Khokhlov, A. M., Oran, E. S., Chtchelkanova, A. Y., & Rosenberg, R. O. 2003, *Science*, 299, 77
- Hillebrandt, W. & Niemeyer, J. C. 2000, *Annu. Rev. Astron. Astrophys.*, 38, 191
- Höflich, P., Wheeler, J. C., & Thielemann, F. K. 1998, *ApJ*, 495, 617
- Khokhlov, A. M. 2000, preprint: astro-ph/0008463
- Leibundgut, B. 2000, *Astron. Astrophys. Rev.*, 10, 179
- Niemeyer, J. C. & Hillebrandt, W. 1995, *Astrophys. J.*, 452, 769
- Osher, S. & Sethian, J. A. 1988, *J. Comp. Phys.*, 79, 12
- Phillips, M. M. 1993, *ApJ*, 413, L105
- Pinto, P. A. & Eastman, R. G. 2000, *ApJ*, 530, 744
- Reinecke, M., Hillebrandt, W., & Niemeyer, J. C. 2002a, *Astron. Astrophys.*, 386, 936
- Reinecke, M., Hillebrandt, W., & Niemeyer, J. C. 2002b, *Astron. Astrophys.*, 391, 1167
- Reinecke, M., Hillebrandt, W., Niemeyer, J. C., Klein, R., & Gröbl, A. 1999, *Astron. Astrophys.*, 347, 724
- Reinecke, M., Niemeyer, J. C., & Hillebrandt, W. 2002c, *New Astronomy Review*, 46, 481
- Timmes, F. X., Brown, E. F., & Truran, J. W. 2003, *ApJ*, 590, L83

- Timmes, F. X. & Woosley, S. E. 1992, *Astrophys. J.*, 396  
Umeda, H., Nomoto, K., Kobayashi, C., Hachisu, I., & Kato,  
M. 1999, *ApJ*, 522, L43